TonB induces conformational changes in surface-exposed loops of FhuA, outer membrane receptor of *Escherichia coli*

KARRON J. JAMES,[1] MARK A. HANCOCK,[2] VIOLAINE MOREAU,[3] FRANCK MOLINA,[3] AND JAMES W. COULTON[1]

[1]Department of Microbiology and Immunology, McGill University, Montreal, Quebec H3A 2B4, Canada
[2]Sheldon Biotechnology Centre, McGill University, Montreal, Quebec H3A 2B4, Canada
[3]FRE 3009 CNRS / Bio-Rad, SysDiag, CAP DELTA, 34184 Montpellier Cedex 4, France

(RECEIVED May 6, 2008; FINAL REVISION July 16, 2008; ACCEPTED July 17, 2008)

Abstract

FhuA, outer membrane receptor of *Escherichia coli*, transports hydroxamate-type siderophores into the periplasm. Cytoplasmic membrane–anchored TonB transduces energy to FhuA to facilitate siderophore transport. Because the N-terminal cork domain of FhuA occludes the C-terminal β-barrel lumen, conformational changes must occur to enable siderophore passage. To localize conformational changes at an early stage of the siderophore transport cycle, four anti-FhuA monoclonal antibodies (mAbs) were purified to homogeneity, and the epitopes that they recognize were determined by phage display. We mapped continuous and discontinuous epitopes to outer surface-exposed loops 3, 4, and 5 and to β-barrel strand 14. To probe for conformational changes of FhuA, surface plasmon resonance measured mAb binding to FhuA in its apo- and siderophore-bound states. Changes in binding kinetics were observed for mAbs whose epitopes were mapped to outer surface-exposed loops. Further, we measured mAb binding in the absence and presence of TonB. After forming immobilized FhuA–TonB complexes, changes in kinetics of mAb binding to FhuA were even more pronounced compared with kinetics of binding in the absence of TonB. Measurement of extrinsic fluorescence of the dye MDCC conjugated to residue 336 in outer surface-exposed loop 4 revealed 33% fluorescence quenching upon ferricrocin binding and up to 56% quenching upon TonB binding. Binding of mAbs to apo- and ferricrocin-bound FhuA complemented by fluorescence spectroscopy studies showed that their cognate epitopes on loops 3, 4, and 5 undergo conformational changes upon siderophore binding. Further, our data demonstrate that TonB binding promotes conformational changes in outer surface-exposed loops of FhuA.

Keywords: monoclonal antibody; phage display; surface plasmon resonance; binding kinetics; fluorescence spectroscopy

Supplemental material: see www.proteinscience.org

Most bacteria require iron to grow, but this element exists predominantly in insoluble forms in the environment, making it difficult to absorb. To acquire iron, bacteria have developed effective transport mechanisms. Bacterial outer membrane (OM) receptors bind and import small molecules called siderophores that chelate iron with high affinity (Ferguson and Deisenhofer 2004).

FhuA, an OM receptor protein of *Escherichia coli*, imports iron chelated by ferrichrome or by its structural analog ferricrocin, both hydroxamate-type siderophores. The iron transport cycle commences when FhuA binds a siderophore. Import of these hydroxamate siderophores through FhuA requires direct contact between FhuA and TonB, a protein anchored in the cytoplasmic membrane

Reprint requests to: James W. Coulton, Department of Microbiology and Immunology, McGill University, 3775 University Street, Montreal, Quebec H3A 2B4, Canada; e-mail: james.coulton@mcgill.ca; fax: (514) 398-7052.

Article and publication are at http://www.proteinscience.org/cgi/doi/10.1110/ps.036244.108.

(CM). At the CM, energy from the proton motive force is harnessed by TonB in complex with ExbB and ExbD and then transduced to FhuA by TonB. To better understand the transport mechanism, whereby *E. coli* acquires iron, molecular details of siderophore import need to be established.

The structure of FhuA is characterized by a C-terminal transmembrane barrel domain composed of 22 antiparallel β-strands connected by long loops on the extracellular surface and short turns on the periplasmic side (Ferguson et al. 1998b; Locher et al. 1998). The interior of the barrel is occluded by an N-terminal globular cork domain. Residues 24–29 of FhuA adopt a helical conformation, referred to as the switch helix. N-terminal to the switch helix of FhuA is the Ton box (residues 7–13), a hepta-peptide motif DTITVTA that displays sequence conservation among OM receptors. Similar structural features were identified in other *E. coli* TonB-dependent OM receptors: FepA (Buchanan et al. 1999), receptor for ferric enterobactin; FecA (Ferguson et al. 2002; Yue et al. 2003), receptor for diferric dicitrate; BtuB (Chimento et al. 2003), receptor for cyanocobalamin; Cir (Buchanan et al. 2007), receptor for colicin Ia; as well as *Pseudomonas aeruginosa* TonB-dependent OM receptors FptA (Cobessi et al. 2005b), receptor for pyochelin; and FpvA (Cobessi et al. 2005a), receptor for pyoverdine.

Structural studies revealed conformational changes at the outer surface of OM receptors. The crystal structure of FecA plus diferric dicitrate shows a change in position of loops 7 and 8 by 11 Å and 15 Å, respectively, compared with their positions in apo-FecA (Ferguson et al. 2002; Yue et al. 2003). In the siderophore-bound conformation, the loops become oriented toward the barrel lumen. Their change in position may prevent siderophore escape into the environment at a later stage of the transport cycle when binding affinity for chelated iron must be reduced to promote its translocation. FepA cross-linking studies (Scott et al. 2002) document structural changes in loop 7 during transport of ferric enterobactin. Comparison of BtuB structures with and without bound cyanocobalamin and Ca^{2+} (Chimento et al. 2003) showed conformational changes in loop 19-20 and in an apical loop of the cork domain. In the cocrystal structure of cyanocobalamin-bound BtuB in complex with TonB (Shultis et al. 2006), a further shift in position of this apical loop was detected. Cocrystal structures of FhuA–TonB (Pawelek et al. 2006) and BtuB–TonB (Shultis et al. 2006) showed structural changes on the periplasmic side of the OM receptors, where formation of an interstrand β-sheet between the Ton box of the receptors and β3 of TonB was observed. Shared architecture of these TonB-dependent OM receptors and their functional similarities suggest that they employ similar mechanisms for translocation of their cognate substrates.

Examining crystal structures of apo- and ferrichrome-bound FhuA (Ferguson et al. 1998b; Locher et al. 1998) and our FhuA–TonB cocrystal structure (Pawelek et al. 2006) did not reveal changes in position of outer surface-exposed loops. However, studies of whole cells indicated conformational changes in residues on loop 4 of FhuA upon binding of ferrichrome (Bos et al. 1998). Given this outcome and the structural changes in outer surface-exposed loops observed in other TonB-dependent transporters, we propose that additional changes may occur at the outer surface of FhuA that have not been revealed by previously adopted methods. In the present study, we report strategies to probe conformational changes in FhuA. By phage display, we mapped monoclonal antibody (mAb) epitopes to specific residues on FhuA. Using surface plasmon resonance (SPR), we measured binding of mAbs to residues on different outer surface-exposed loops of FhuA in the absence and presence of both ferricrocin and TonB. By use of fluorescence spectroscopy, we measured quenching at residue 336 in the outer surface-exposed loop 4 of FhuA upon ferricrocin binding and upon TonB binding. Our findings provide evidence that TonB induces conformational changes in outer surface-exposed loops of FhuA.

Results and Discussion

Mapping of mAb epitopes

To use mAbs as probes of conformational changes, four anti-FhuA mAbs were purified to homogeneity from tissue culture supernatants by immunoaffinity chromatography. Purity (>95%) of each mAb was confirmed by SDS-PAGE with silver staining, and in all cases, a band at ~50 kDa corresponding to the heavy chain and another at ~25 kDa corresponding to the light chain were observed. To identify minimum FhuA epitopes, a Ph.D.-12 phage-displayed combinatorial peptide library was panned against each mAb. FhuA epitopes were determined for three mAbs using the RELIC/MATCH bioinformatics program (Table 1; Fig. 1), which performed pairwise alignments between the amino acid sequence of FhuA and each affinity-selected peptide. We previously mapped (Moeck et al. 1995) the mAb Fhu4.1 epitope to an outer surface-located region, residues 321–381. Consistent with this result, panning against this mAb significantly narrowed these boundaries, establishing residues 332–336 (LAPAD) on extracellular surface loop 4 as its cognate epitope. Peptides selected from panning against mAbs Fhu6.4 and Fhu6.6 mapped to residues 533–536 (refined from 417–550) on transmembrane strand 14 of the β-barrel.

MAb Fhu3.1, predicted to bind to a discontinuous epitope (Moeck et al. 1995), was also panned against the Ph.D.-12 library. Thirty unique peptides were affinity

Table 1. *Anti-FhuA mAb affinity-selected peptides mapped to FhuA*

mAb (isotype)[a]	Peptides[b]	Peptide MATCH score[c]	Location of epitope
	(325) YSKQCAA**LAPAD**KGHYL (341)[d]		
Fhu4.1	tpls**lapad**qwl	20	loop 4
(IgG1)	wv**lapad**rarsl	20	
	fd**lapad**rnwgs	20	
	qdlt**lapad**yla	20	
	smqahlr**lapad**	20	
	tqhlt*m***apad**sk	17	
	mhqt**l***s***pad**lat	17	
	allcdw**apad**cs	15	
	(526) KGKQYE*V***GVKY**VP**E**DR (541)		
Fhu6.4	sq*l***gvky**hmpgs	17	β-strand 14
(IgG1)	qtgg*l***gvky**frv	17	
	qtqt*l***gvky**fr**e**	17	
	yaqy**gvky**kt**e**t	16	
	yfndvq*l***gv***r***y**h	14	
	lpst*is***vky**hst	13	
	(527) GK**Q**Y**E***V***GVKY**VPEDRP (542)		
Fhu6.6	fpvhn*l***gv***r***y**pg	14	β-strand 14
(IgG1)	dpdq*l***gv***r***y**hka	14	
	e*l***gvn****y**ysatsr	13	
	s**q**t*dls***vky**yns	13	

[a] See Moeck et al. (1995).
[b] Residues in bold represent exact matches to FhuA (PDB code 1FCP); italicized residues represent conserved substitutions. Peptides selected from Ph.D.-12 Phage Display Peptide Library (NEB) and aligned using RELIC/MATCH (http://relic.bio.anl.gov).
[c] Modified BLOSUM62 matrix used for scoring.
[d] Uppercase underlined residues represent regions primary sequence of FhuA (PDB code 1FCP); numbers in parentheses represent amino acid boundaries.

selected and then analyzed using the MIMOP bioinformatics suite (Moreau et al. 2006), which includes three tools: MimAlign, MimCons, and a combined method. MimAlign and the combined method both identified the epitope for mAb Fhu3.1 that includes amino acids W246 V253 P255 P257 N258 K260 R261 P263 within loop 3 and residues Y403 N404 N416 T417 D418 within loop 5 (Fig. 1).

MAb binding kinetics altered by ferricrocin and by TonB

To investigate mAb binding to FhuA in the absence and presence of ferricrocin and of TonB, real-time binding kinetics were monitored using SPR. By SDS-PAGE followed by silver staining, purity of all preparations of FhuA and TonB (>95%) was confirmed. By immunoblotting and ELISA, we determined that mAbs were specific only for FhuA; they were not reactive toward TonB.

For SPR assays with TonB, immobilization of mAbs followed by injection of TonB alone led to nonspecific binding of TonB to reference surfaces. Hence, TonB was immobilized to sensor chips followed by injection of FhuA and then mAbs. Alternatively, FhuA was tethered by its N terminus using mAb Fhu8.3 (Moeck et al. 1995), that recognizes residues 1–7 at the N terminus of FhuA (see Supplemental material). TonB is known (Bell et al. 1990; Moeck et al. 1997; Coggshall et al. 2001; Howard et al. 2001; Moeck and Letellier 2001; Pawelek et al. 2006) to bind the Ton box of OM receptors. To further verify that TonB bound only to the periplasmic face of FhuA, mAb Fhu8.3 was injected over immobilized FhuA–TonB complexes. MAb binding was not detected, indicating that the Fhu8.3 epitope was engaged by TonB on all FhuA molecules. Thus, use of TonB or mAb Fhu8.3 to capture FhuA provided a similar orientation of FhuA to ensure that changes in mAb binding to FhuA, tethered by a physiologically relevant ligand (TonB) compared with mAb binding to FhuA, tethered by a physiologically irrelevant ligand (mAb Fhu8.3), were due to the presence of bound TonB.

Conformational changes of antigens based on properties of mAb binding have been previously investigated using SPR (Zhang et al. 2001; Bowlby et al. 2005). Guided by these reports, TonB (100–200 resonance units [RU]) was thiol-coupled to sensor chip surfaces at its N terminus, thereby orienting the capture of FhuA (50–200 RU) to mimic the spatial relationship of these two proteins in the bacterial cell envelope. MAbs Fhu4.1 and Fhu3.1, both with epitopes located on the extracellular surface of FhuA, were then injected over reference surfaces (TonB) and test surfaces (TonB + FhuA). For assays in the absence of TonB, 1800 RU of anti-FhuA mAb

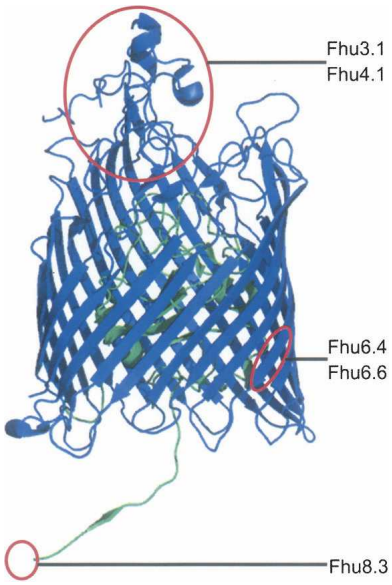

Figure 1. Anti-FhuA mAb epitopes mapped by phage display to FhuA (PDB code 2GRX; TonB removed for clarity; residues 1–7 were not resolved in the crystal structure). Affinity-selected peptides analyzed using RELIC and MIMOP. FhuA cork domain is shown in green; barrel domain is shown in blue. Highlighted in red circles are mAbs mapping to outer surface-exposed loops: Fhu3.1 and Fhu4.1, to the N terminus: Fhu8.3; and to β-strand 14: Fhu6.4, Fhu6.6. Ribbon representation of FhuA generated using PyMOL (http://www.pymol.org).

Fhu8.3 was amine-coupled to sensor chips followed by capture of FhuA (50–200 RU) at its N terminus. Having demonstrated that binding of FhuA by the capture antibody was unaltered by ferricrocin (data not shown), the following analytes were then injected over reference (mAb Fhu8.3) and over test surfaces (mAb Fhu8.3 + FhuA): mAbs Fhu4.1 and Fhu3.1. For all assays, specific and dose-dependent binding of mAbs to apo- or siderophore-bound FhuA surfaces was observed (Figs. 2, 3). Predicted K_D values (Table 2) indicated a range of low nanomolar affinities (1.2–18 nM) for mAbs Fhu4.1 and Fhu3.1 binding to their FhuA epitopes.

For mAb Fhu4.1, its apparent rates of association (k_a) with FhuA decreased 1.5- to twofold compared with its binding to FhuA–TonB (Table 2). Apparent rates of mAb dissociation (k_d) from FhuA–TonB complexes showed 1.5-fold differences in the absence of ferricrocin compared with dissociation from the complex in the presence of ferricrocin (Table 2; Fig. 2). The most striking difference in mAb binding kinetics for Fhu4.1 was demonstrated by its six times faster rate of dissociation from FhuA–TonB complexes with bound ferricrocin (32×10^{-4}/sec) compared with its rate of dissociation from FhuA plus ferricrocin (5.2×10^{-4}/sec; Table 2). These changes in kinetic parameters show continued access by Fhu4.1 to its epitope upon ferricrocin and TonB binding. Ferricrocin and TonB binding likely induced changes in accessibility of epitopic residues that affected the apparent rate of association of mAb with FhuA. Induced changes would influence the structure of the mAb–FhuA binding interface and, in turn, the apparent rate of dissociation of mAb from FhuA. Significantly, our outcomes demonstrate that binding of FhuA to immobilized TonB reduces the overall affinity of Fhu4.1 for its epitope compared to mAb affinity for FhuA in the absence of TonB. We interpret these observations as conformational changes in extracellular loop 4 residues (332–336, LAPAD) that are recognized by mAb Fhu4.1.

Moeck et al. (1997) determined that mAbs Fhu6.4 and Fhu6.6 were not surface reactive; they gave positive reactions only by Western blotting versus denatured FhuA. Our phage panning results (Table 1) now show that these mAbs recognize a transmembrane epitope located on β-strand 14. As negative controls in our SPR assays, mAbs Fhu6.4 and Fhu6.6 (each at 100 nM) were injected over FhuA surfaces; low binding responses (0–5 RU) were observed, consistent with the location of epitopes for these mAbs.

In the absence of ferricrocin, we observed faster mAb Fhu3.1 dissociation from FhuA–TonB (11×10^{-4}/sec; Table 2) than from FhuA alone (4×10^{-4} /sec; Table 2). In the presence of ferricrocin, k_a for mAb Fhu3.1 binding to FhuA (23×10^4/Msec) (Table 2) versus its binding to FhuA–TonB complexes (45×10^4/Msec; Table 2) illustrated its faster rate of binding following FhuA–TonB complex formation. Apparent k_d showed twofold faster mAb dissociation from FhuA–TonB complexes in the absence of ferricrocin than in the presence of ferricrocin (11×10^{-4} /sec vs. 5.5×10^{-4} /sec, respectively; Table 2; Fig. 3). These outcomes show that FhuA–TonB binding promotes conformational changes in outer surface-exposed loops 3 and 5 of FhuA. Additionally, our data indicate that the presence of ferricrocin may alter the properties of FhuA–TonB binding, thereby modifying the conformational changes that occur upon complex formation.

Repetition of the highest analyte concentration at the start and end of each titration series validated reproducibility of our assays. Binding responses for replicate injections agreed within 2 RU on average. All data were analyzed globally using the bivalent analyte model (DiGiacomo et al. 2004). χ^2 values were all <1. These values along with residual plots establish the goodness of fit of the data, and reported standard errors validate their statistical significance.

Residue 336 in loop 4 undergoes conformational changes in response to binding of ferricrocin and of TonB

To extend these studies on conformational changes in FhuA, we measured changes in extrinsic fluorescence emission of FhuA(D336C) labeled with the thiol-specific

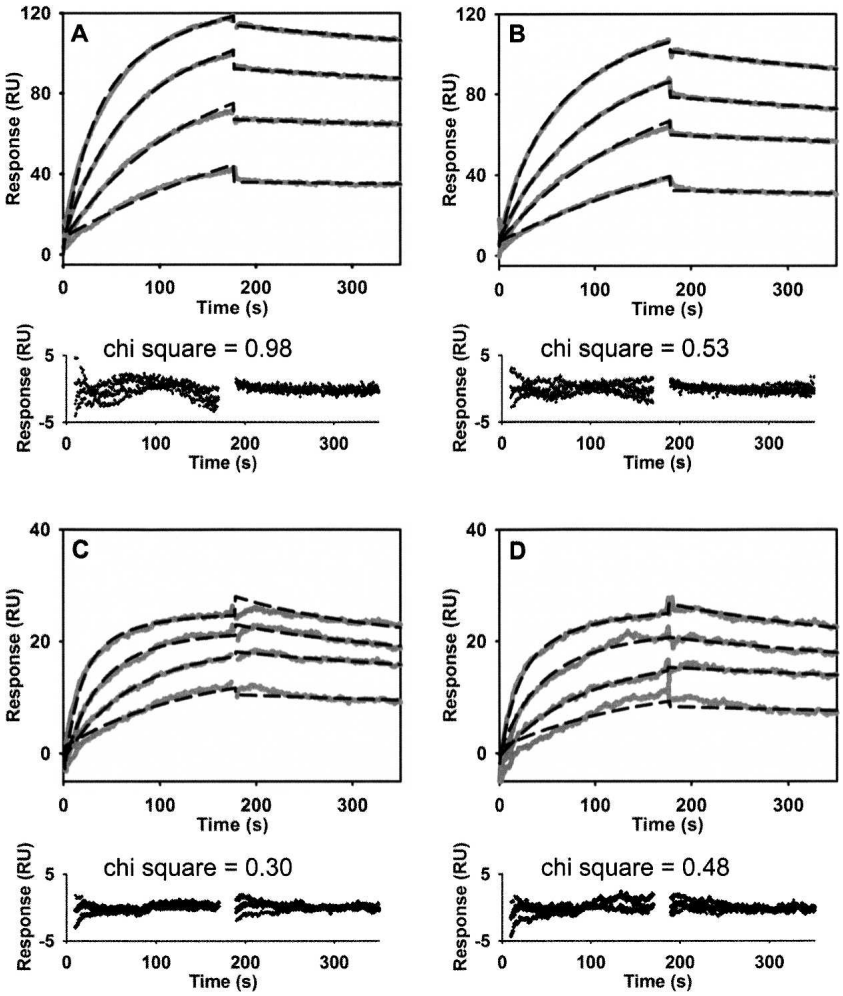

Figure 2. SPR analysis of mAb Fhu4.1 binding to FhuA. MAb Fhu4.1 (10, 25, 50, 100 nM) binding to 200 RU apo- FhuA (*A*) or to ferricrocin-bound FhuA (*B*), both in the absence of TonB (i.e., 2000 RU amine-coupled mAb Fhu8.3 for capture). MAb Fhu4.1 (10, 25, 50, 100 nM) binding to 100 RU apo-FhuA (*C*) or to ferricrocin-bound FhuA (*D*), both in the presence of TonB (i.e., 200 RU thiol-coupled TonB for capture). Solid gray lines represent the raw data; black dashed lines represent mathematical curve-fitting according to the bivalent analyte model (BIAevaluation version 4.1). χ^2 values and plots of residuals are shown *below* each panel.

fluorophore MDCC. Fluorescence emission by MDCC is affected by changes in polarity of its immediate environment. We avoided use of a reducing agent in the labeling protocol to prevent reduction of the two native disulfide linkages in FhuA, thereby ensuring that only the free cysteine at residue 336 in outer surface-exposed loop 4 was amenable to labeling by MDCC. In studies reported by Eisenhauer et al. (2005), residue 336 on FhuA(D336C) was labeled by thiol-specific fluorescent probe Oregon green maleimide. In the present work, we conjugated MDCC to the free cysteine residue in FhuA(D336C) and achieved a coupling efficiency of 1 mole of dye for each mole of protein. To ensure loading of FhuA with ferricrocin, a 10-fold molar excess of ferricrocin was added to FhuA(D336C). This addition resulted in a considerable decrease in emission maxima relative to fluorescence emissions of FhuA(D336C-MDCC) alone (Fig. 4): 33% fluorescence quenching was observed. Such an outcome is consistent with results from previous studies (Bos et al. 1998) showing that addition of ferrichrome to bacterial cells expressing FhuA labeled with fluorescein maleimide led to a decrease in fluorescence emission. Our present study has further exploited this approach to investigate the effects of FhuA–TonB complex formation. Addition of TonB to FhuA(D336C-MDCC) in a 1:1 molar ratio resulted in a marked 48% fluorescence quenching (Fig. 4). Titration of TonB (0.5 to 10 μM) into FhuA(D336C-MDCC) identified a concentration-dependent decrease in emission of extrinsic fluorescence from 5% to 56%. As negative controls, addition of 2 μM BSA or of buffer alone to FhuA(D336C-MDCC) produced emission spectra that were almost coincident with those of FhuA(D336C-MDCC) alone.

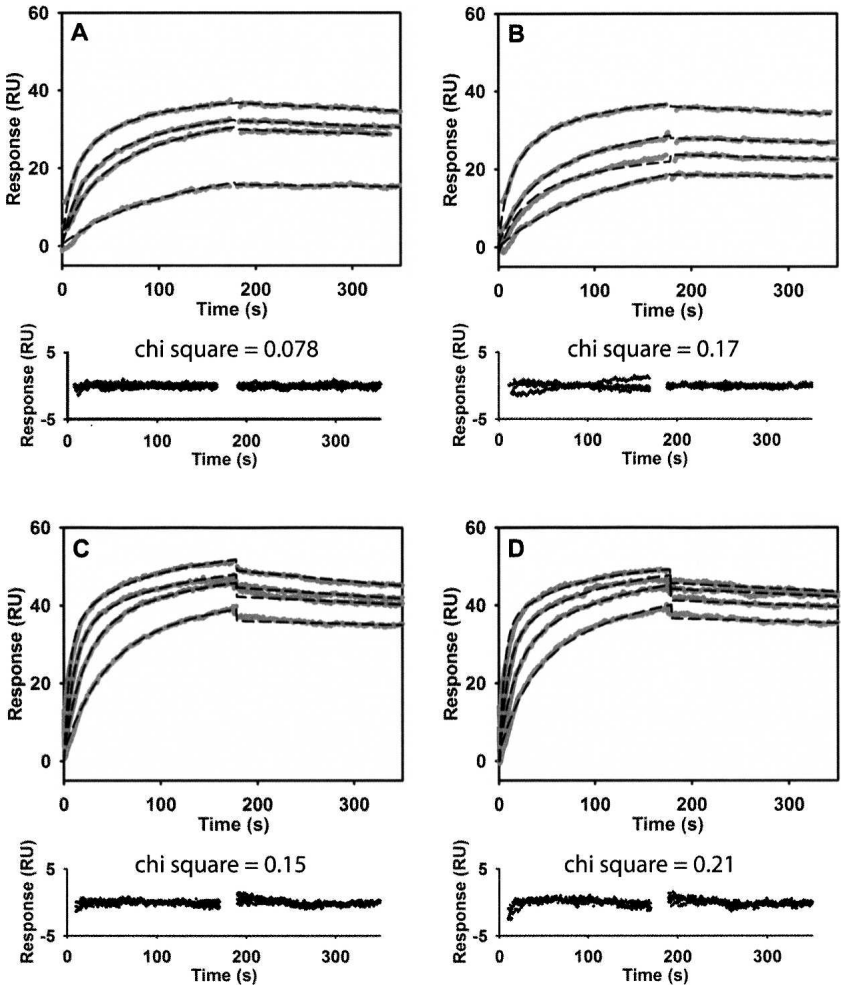

Figure 3. SPR analysis of mAb Fhu3.1 binding to FhuA. MAb Fhu3.1 (10, 30, 50, 100 nM) binding to 50 RU apo-FhuA (*A*) or to ferricrocin-bound FhuA (*B*), both in the absence of TonB (i.e., 1800 RU amine-coupled mAb Fhu8.3 for capture). MAb Fhu3.1 (10, 30, 50, 100 nM) binding to 150 RU apo-FhuA (*C*) or to ferricrocin-bound FhuA (*D*), both in the presence of TonB (i.e., 100 RU thiol-coupled TonB for capture). Solid gray lines represent the raw data; black dashed lines represent mathematical curve-fitting according to a bivalent analyte model (BIAevaluation version 4.1). χ^2 values and plots of residuals are shown *below* each panel.

Taken together, our SPR and fluorescence studies indicate that FhuA outer surface-exposed loop 4 undergoes TonB-dependent changes in conformation in addition to changes induced by ferricrocin. Although at this time we cannot exclude the possibility that conformational changes in nearby loops affect accessibility of mAb Fhu4.1 for its epitope, in vivo and in vitro studies have also advocated the importance of loop 4 in ferrichrome binding and transport (Killmann et al. 1993; Braun et al. 1994); the LAPAD sequence was previously (Killmann et al. 1995) shown to play some role in TonB-dependent uptake of phage ϕ-80. By demonstrating measurable changes in mAb Fhu4.1 binding after FhuA and TonB form a complex, our data substantiate the importance of this sequence in outer surface-exposed loop 4.

Our previous measurements of FhuA–TonB binding kinetics by SPR (Khursigara et al. 2004, 2005) demonstrated an interaction best described by a two-state conformational rearrangement model. Assays using both TonB 32–239 and a C-terminal construct TonB 155–239 indicated formation of an initial lower affinity complex with FhuA and a subsequent higher affinity complex that was enhanced by the presence of ferricrocin. These studies identified a twofold increase in stability of a FhuA–TonB complex in the presence of ferricrocin compared with stability of the complex in the absence of ferricrocin. From our current SPR and fluorescence data, we conclude that binding of both ferricrocin and TonB leads to conformational changes of residue 336 of outer surface-exposed loop 4 of FhuA. Although enhancement of quenching by the addition of TonB to FhuA plus

Table 2. *Apparent kinetics of mAb binding to apo- and ferricrocin-loaded FhuA or FhuA–TonB complexes, as assessed by* SPR[a]

mAb	Predicted epitope on FhuA		FhuA − ferricrocin[b]			FhuA + ferricrocin		
			$k_a \times 10^4$ (1/Msec)	$k_d \times 10^{-4}$ (1/sec)	K_D (nM)	$k_a \times 10^4$ (1/Msec)	$k_d \times 10^{-4}$ (1/sec)	K_D (nM)
Fhu4.1	Loop 4	−TonB	9.1 ± 0.09	11 ± 0.4	9.7 ± 0.4	8.4 ± 0.1	5.2 ± 0.3	5.0 ± 0.3
		+TonB	17 ± 0.4	19 ± 2	11 ± 0.8	13 ± 0.2	32 ± 0.9	18 ± 0.6
Fhu3.1	Loops 3, 5	−TonB[c]	30 ± 0.2	4.0 ± 0.3	1.4 ± 0.1	23 ± 0.9	3.8 ± 0.5	1.3 ± 0.2
		+TonB[d]	41 ± 0.5	11 ± 0.8	2.5 ± 0.2	45 ± 0.7	5.5 ± 0.3	1.2 ± 0.06

[a] Estimates for the first association and dissociation rate constants are reported.
[b] Values representative of three independent experiments ± SE.
[c] FhuA captured by immobilized antibody then binding of mAbs in column 1 measured.
[d] FhuA captured by immobilized TonB then binding of mAbs in column 1 measured.

ferricrocin, beyond that observed in the absence of ferricrocin was not evident, we propose that the presence of ferricrocin leads to conformational changes in other residues of FhuA that promote binding by TonB.

Binding of ferricrocin to FhuA was shown to trigger unwinding of its switch helix (Ferguson et al. 1998b; Locher et al. 1998), an event that may signal receptor occupancy to TonB. Recently, site-directed spin labeling studies (Kim et al. 2007) indicated that the switch helix of FhuA and of FecA is unwound even in the absence of siderophore, implying that there may be a different recruitment signal for TonB. The cocrystal complex of Shultis et al. (2006) demonstrated that binding of TonB induces conformational change in an apical loop of the cork domain of BtuB. Changes in outer surface-exposed loops of the barrel domain were attributed to the crystallization process. The present study provides new details regarding conformational changes in FhuA outer surface-exposed loops 3, 4, and 5 of the barrel domain by identifying changes in apparent mAb binding kinetics for apo-FhuA versus siderophore-bound FhuA. In our model of siderophore transport, extension of the FhuA N terminus into the periplasm not only facilitates interaction at multiple sites between FhuA and TonB (Killmann et al. 2002; Khursigara et al. 2005; Pawelek et al. 2006) but also induces changes in extracellular regions of FhuA. More strikingly, conformational changes of epitopic residues in loops 3, 4, and 5 as measured by real-time apparent kinetics of mAb binding to apo- and siderophore-bound FhuA and by fluorescence spectroscopy were promoted by the presence of bound TonB. The differences in apparent kinetic parameters measured by SPR are consistent with structural changes that were not evident in the FhuA–TonB cocrystal structure (Pawelek et al. 2006), a static representation. Loops 4 and 5, the longest loops on FhuA, may be involved in a gating mechanism as identified for loops 7 and 8 in FecA (Ferguson et al. 2002), and as suggested for loop 8 in FhuA (Faraldo-Gomez et al. 2003), to prevent diffusion of substrate into the extracellular environment. Movement of the epitopic residues signals a change in the molecular architecture of the mAb binding regions that decreases affinity of ferricrocin for its initial binding site on FhuA, thus promoting siderophore import. Hence, conformational changes in extracellular loops play a measurable and demonstrable role in the siderophore transport cycle of this OM receptor. Binding kinetics of loop residues of other OM receptors at different stages of the cycle will elucidate commonalities in their transport mechanisms.

Materials and Methods

Strains and culture conditions

E. coli K-12 strain AW740 (*hisG4 thr-1 fhuA31 tsx-78* Δ*ompF zcb*::Tn*10* Δ*ompC*) harbors plasmid pHX405 that expresses recombinant FhuA; at residue 405, a hexa-histidine tag is flanked by five linker residues (Moeck et al. 1996). The *fhuA* gene was engineered (Eisenhauer et al. 2005) to produce the single residue change D336C on outer surface-exposed loop 4. Bacteria were grown for 16 h in M63 minimal glucose medium with shaking at 37°C. For phage propagation, *E. coli* ER2738 (New England BioLabs [NEB]) was grown at 37°C to mid-log

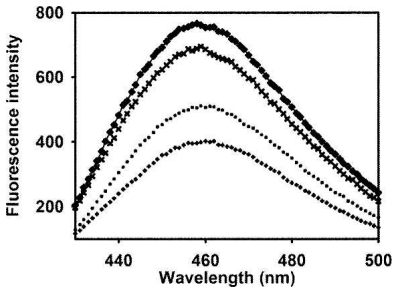

Figure 4. Fluorescence quenching of MDCC-labeled FhuA(D336C). Fluorescence emission maxima of 1 μM FhuA(D336C) (◆); FhuA(D336C) plus 1 μM TonB (+); FhuA(D336C) plus 10 μM ferricrocin (+); and FhuA(D336C) plus 10 μM ferricrocin plus 1 μM TonB (+). Plots are representative of three independent assays.

phase in Luria Bertani (LB) broth supplemented with tetracycline (20 μg/mL). *E. coli* ER2566/pCMK01 expresses TonB residues 32–239 and includes an introduced cysteine at its N terminus (Khursigara et al. 2005). Expression of TonB was induced with 0.5 mM isopropyl-β-D-thiogalactopyranoside (IPTG); cells were grown in LB broth at 30°C for 4 h post-induction.

Protein purification

E. coli cells overexpressing genes for recombinant FhuA and variant FhuA(D336C) were lysed using a modified lysozyme/EDTA protocol (Hantke 1981). Isolated OM proteins were solubilized in dimethyldodecylamine-N-oxide (LDAO; Fluka) and were purified as previously described (Ferguson et al. 1998a). For TonB extraction, *E. coli* cells were exposed to lysozyme for 30 min at room temperature. Spheroplasts were lysed on ice by an Emulsiflex-C5 homogenizer (Avestin), two cycles at 16,000 psi. Soluble cell extract was purified as previously described (Khursigara et al. 2004). Purity of FhuA variants and TonB was assessed by SDS-PAGE (10% polyacrylamide gels) under nonreducing and reducing (5% [v/v] 2-mercaptoethanol) conditions followed by silver staining (750 ng protein/lane). Protein concentrations were determined using BCA assay (Pierce).

Antibody purification

Mouse mAbs raised against detergent-solubilized FhuA (Moeck et al. 1995) were immunoaffinity-purified from tissue culture supernatants as follows. Rat anti-mouse κ light chain mAb P187.1 (Yelton et al. 1981) was coupled to cyanogen bromide-activated Sepharose 4 Fast Flow beads (Amersham Biosciences) according to the manufacturer's instructions. Protein coupling was quantitatively monitored by dye-binding assays (Bio-Rad). For immunoaffinity purification, tissue culture supernatants were adjusted to pH 8.0 with 1 M Tris pH 8.5 and applied to the P187.1-immobilized resin equilibrated in phosphate-buffered saline (PBS). MAbs were eluted with 0.2 M glycine-HCl pH 3.0 and the solution immediately neutralized with 0.1 M Tris pH 8.5. The mAbs were purified to homogeneity as assessed by SDS-PAGE analysis (12% polyacrylamide) under nonreducing and reducing (5% [v/v] 2-mercaptoethanol) conditions followed by silver staining (500 ng protein/lane). Purified mAbs were quantified by dye-binding assays (Bio-Rad).

Phage display

Epitope mapping of anti-FhuA mAbs was performed using the Ph.D.-12 Phage Display Peptide Library (NEB), a combinatorial library of M13 phages that displays three to five copies of a random 12-residue linear peptide fused to the N terminus of pIII coat proteins. For each target mAb, 15 μg in 0.1 M sodium bicarbonate solution pH 8.6 was incubated overnight at 4°C in a micro-well (Nunc Maxisorp). Phage panning was performed as described previously (Carter et al. 2006a). Phage eluates were amplified in *E. coli* ER2738 culture for 4.5 h at 37°C and purified using polyethylene glycol-8000 in 2.5 M sodium chloride. Eluates were titered and 10^{10} pfu used as input for subsequent rounds of panning. Three rounds of affinity selection were performed for each mAb. From clones selected after the third round of panning, phage DNA was purified using QIAprep 96 M13 Kit (Qiagen). If sequence diversity after three rounds of panning was apparently low, phage clones were selected from round 2 eluates. Purified M13 phage DNA was subjected to sequencing at McGill University's Sheldon Biotechnology Center (SBC) or the McGill University and Génome Québec Innovation Center.

Analysis of affinity-selected peptides

Peptide sequences derived from M13 DNA were evaluated by REceptor LIgand Contacts (RELIC; http://relic.bio.anl.gov) (Mandava et al. 2004) bioinformatics suite. The RELIC/MATCH program enabled pairwise alignments between the FhuA sequence and that of affinity-selected peptides. MAbs whose epitopes were previously (Moeck et al. 1995) determined to be discontinuous in nature were mapped to FhuA using MIMOP (http://www.sysdiag.cnrs.fr/MIMOP/) (Moreau et al. 2006). The MIMOP suite is a computational tool predicting continuous or discontinuous epitopes from mimotope peptide sequences. On the one hand (MimAlign approach), MIMOP was used to analyze the global similarity of the peptide sequences to the antigen sequence by exploiting multiple sequence alignments performed by four different algorithms. On the other hand (MimCons approach), MIMOP was used to analyze the peptide sequences to identify key residues on the antigen surface. MimAlign and MimCons results were combined to give convergent predictions: a list of solvent-exposed residues comprising the epitope of the antigen. MIMOP default parameters were used for epitope mapping, except for mAb Fhu3.1 where the DCA (Stoye et al. 1997) program was deselected to facilitate data analysis.

Surface plasmon resonance

Binding interactions between anti-FhuA mAbs (~150 kDa) and FhuA (79 kDa) were examined in real time using Biacore 2000/3000 instrumentation (GE Healthcare Bio-Sciences AB). Experiments were performed on research-grade CM4 sensor chips at 25°C using filtered (0.2 μm) and degassed HBS-T running buffer (50 mM HEPES pH 7.4, 150 mM NaCl, 0.05% [v/v] Tween 20 [Calbiochem]). FhuA was dialyzed against the running buffer prior to SPR experiments. For all binding assays conducted in the presence of siderophore, a 10-fold molar excess of ferricrocin (1.0 μM) was added to FhuA (100 nM) and incubated for 30 min at room temperature (Khursigara et al. 2004). After FhuA was injected, unbound siderophore was removed by extensive washing.

To measure mAb binding to FhuA bound to TonB, TonB (25 kDa; 10 μg/mL in 10 mM sodium acetate pH 4.0) was thiol-coupled to sensor chips. Corresponding reference surfaces were prepared in a similar manner. For test surfaces, FhuA was diluted in HBS-T and captured at 20 μL/min (40-sec injections) over the immobilized TonB surfaces. After 30-sec washes with NaCl (0.5 M) and HBS-T, diluted mAbs were injected (180 sec association + 180 sec dissociation) over reference (TonB) and test (TonB + FhuA) surfaces. Regeneration of immobilized TonB surfaces was achieved using regeneration schemes I and II: scheme I, 25-sec injection of acids/chaotropes/EDTA cocktail (Andersson et al. 1999) followed by 25-sec injection of running buffer; scheme II, two 25-sec injections each of acids/chaotropes/EDTA cocktail, 0.1% (v/v) dodecyl-β-D-maltoside, 0.1% (v/v) Triton X-100, 0.1% (v/v) Empigen, and HBS-T, in sequence. Each detergent (Calbiochem) was diluted in HBS-T to achieve the indicated concentration.

For comparison, we measured binding of mAbs to FhuA that was tethered by a physiologically irrelevant binding partner mAb Fhu8.3 (10 μg/mL in 10 mM sodium acetate pH 5.0) amine coupled to sensor chips. Assays were conducted as described above for mAb binding measurements in the presence of TonB. By tests of various flow rates (Quinn and O'Kennedy 2001; Drake et al. 2004) mass transport effects were excluded.

All SPR data are representative of injections acquired from three independent trials. As recommended by the manufacturer, a buffer blank was injected first, the highest analyte concentration second, and serial dilutions then followed (from the lowest to the highest concentration repeated). Comparing binding responses between the highest analyte injections verified consistent immobilized-surface activity throughout each assay. Binding data were double-referenced (Myszka 1999) and analyzed globally according to the bivalent analyte model in BIAevaluation version 4.1 software:

$$L1 + A1 \overset{k_{a1}, k_{d1}}{\longleftrightarrow} L1A1 \quad (1)$$

$$L1A1 + L2 \overset{k_{a2}, k_{d2}}{\longleftrightarrow} L1A1L2, \quad (2)$$

where L and A correspond to ligand and analyte, respectively; k_{a1} has units of $M^{-1}sec^{-1}$; k_{d1} has units of sec^{-1}; k_{a2} has units of $RU^{-1}sec^{-1}$; and k_{d2} has units of sec^{-1}. The first apparent association rate constant is dependent on the concentration of injected mAb, whereas k_{a2} is dependent on the number of available ligand binding sites remaining after the first binding event. Apparent affinities (K_D) were calculated using estimates for the first association (k_{a1}) and dissociation (k_{d1}) rate constants ($K_D = k_{d1}/k_{a1}$) (DiGiacomo et al. 2004). Evaluations were performed using local R_{max} parameters to account for cycle-to-cycle variations in the amount of FhuA captured between sample injections.

Fluorescence spectroscopy

The fluorophore 7-diethylamino-3-((((2-maleimidyl)-ethyl)amino) carbonyl)coumarin (MDCC) was purchased from Invitrogen. MDCC was conjugated to FhuA(D336C) in 50 mM HEPES pH 7.4, 150 mM NaCl, and 0.05% Tween 20, and fluorescence emissions were measured as previously described (Carter et al. 2006b). Measurements were taken in triplicate at 20°C. Data were corrected for changes in fluorescence intensity due to dilution of protein and for minimal fluorescence contributions of ferricrocin, TonB, and buffer. Fluorescence emissions were measured for binding of ferricrocin (10 μM), TonB (up to 10-fold molar excess), and BSA (negative control) to FhuA (1 μM).

Acknowledgments

We thank H. Brum for contribution of experimental materials, C. Ng-Thow-Hing for bioinformatics support, and D.M. Carter and J. Deme for technical support. This work was supported by operating grants to J.W.C. from the Canadian Institutes of Health Research (CIHR). Sheldon Biotechnology Centre is supported by a Research Resource Grant from CIHR. Canada Foundation for Innovation provided infrastructure for surface plasmon resonance to the Montreal Integrated Genomics Group for Research on Infectious Pathogens. K.J.J. is a recipient of scholarships from the Organization of American States and from the Canadian Commonwealth Scholarships Program.

References

Andersson, K., Hamalainen, M., and Malmqvist, M. 1999. Identification and optimization of regeneration conditions for affinity-based biosensor assays. A multivariate cocktail approach. *Anal. Chem.* **71:** 2475–2481.

Bell, P.E., Nau, C.D., Brown, J.T., Konisky, J., and Kadner, R.J. 1990. Genetic suppression demonstrates interaction of TonB protein with outer membrane transport proteins in *Escherichia coli*. *J. Bacteriol.* **172:** 3826–3829.

Bos, C., Lorenzen, D., and Braun, V. 1998. Specific in vivo labeling of cell surface-exposed protein loops: Reactive cysteines in the predicted gating loop mark a ferrichrome binding site and a ligand-induced conformational change of the *Escherichia coli* FhuA protein. *J. Bacteriol.* **180:** 605–613.

Bowlby, M.R., Chanda, P., Edris, W., Hinson, J., Jow, F., Katz, A.H., Kennedy, J., Krishnamurthy, G., Pitts, K., Ryan, K., et al. 2005. Identification and characterization of small molecule modulators of KChIP/Kv4 function. *Bioorg. Med. Chem.* **13:** 6112–6119.

Braun, V., Killmann, H., and Benz, R. 1994. Energy-coupled transport through the outer membrane of *Escherichia coli* small deletions in the gating loop convert the FhuA transport protein into a diffusion channel. *FEBS Lett.* **346:** 59–64.

Buchanan, S.K., Smith, B.S., Venkatramani, L., Xia, D., Esser, L., Palnitkar, M., Chakraborty, R., van der Helm, D., and Deisenhofer, J. 1999. Crystal structure of the outer membrane active transporter FepA from *Escherichia coli*. *Nat. Struct. Biol.* **6:** 56–63.

Buchanan, S.K., Lukacik, P., Grizot, S., Ghirlando, R., Ali, M.M., Barnard, T.J., Jakes, K.S., Kienker, P.K., and Esser, L. 2007. Structure of colicin I receptor bound to the R-domain of colicin Ia: Implications for protein import. *EMBO J.* **26:** 2594–2604.

Carter, D.M., Gagnon, J.N., Damlaj, M., Mandava, S., Makowski, L., Rodi, D.J., Pawelek, P.D., and Coulton, J.W. 2006a. Phage display reveals multiple contact sites between FhuA, an outer membrane receptor of *Escherichia coli*, and TonB. *J. Mol. Biol.* **357:** 236–251.

Carter, D.M., Miousse, I.R., Gagnon, J.N., Martinez, E., Clements, A., Lee, J., Hancock, M.A., Gagnon, H., Pawelek, P.D., and Coulton, J.W. 2006b. Interactions between TonB from *Escherichia coli* and the periplasmic protein FhuD. *J. Biol. Chem.* **281:** 35413–35424.

Chimento, D.P., Mohanty, A.K., Kadner, R.J., and Wiener, M.C. 2003. Substrate-induced transmembrane signaling in the cobalamin transporter BtuB. *Nat. Struct. Biol.* **10:** 394–401.

Cobessi, D., Celia, H., Folschweiller, N., Schalk, I.J., Abdallah, M.A., and Pattus, F. 2005a. The crystal structure of the pyoverdine outer membrane receptor FpvA from *Pseudomonas aeruginosa* at 3.6 Å resolution. *J. Mol. Biol.* **347:** 121–134.

Cobessi, D., Celia, H., and Pattus, F. 2005b. Crystal structure at high resolution of ferric-pyochelin and its membrane receptor FptA from *Pseudomonas aeruginosa*. *J. Mol. Biol.* **352:** 893–904.

Coggshall, K.A., Cadieux, N., Piedmont, C., Kadner, R.J., and Cafiso, D.S. 2001. Transport-defective mutants alter the conformation of the energy-coupling motif of an outer membrane transporter. *Biochemistry* **40:** 13964–13971.

DiGiacomo, R.A., Xie, L., Cullen, C., and Indelicato, S.R. 2004. Development and validation of a kinetic assay for analysis of anti-human interleukin-5 monoclonal antibody (SCH 55700) and human interleukin-5 interactions using surface plasmon resonance. *Anal. Biochem.* **327:** 165–175.

Drake, A.W., Myszka, D.G., and Klakamp, S.L. 2004. Characterizing high-affinity antigen/antibody complexes by kinetic- and equilibrium-based methods. *Anal. Anal. Biochem.* **328:** 35–43.

Eisenhauer, H.A., Shames, S., Pawelek, P.D., and Coulton, J.W. 2005. Siderophore transport through *Escherichia coli* outer membrane receptor FhuA with disulfide-tethered cork and barrel domains. *J. Biol. Chem.* **280:** 30574–30580.

Faraldo-Gomez, J.D., Smith, G.R., and Sansom, M.S. 2003. Molecular dynamics simulations of the bacterial outer membrane protein FhuA: A comparative study of the ferrichrome-free and bound states. *Biophys. J.* **85:** 1406–1420.

Ferguson, A.D. and Deisenhofer, J. 2004. Metal import through microbial membranes. *Cell* **116:** 15–24.

Ferguson, A.D., Breed, J., Diederichs, K., Welte, W., and Coulton, J.W. 1998a. An internal affinity-tag for purification and crystallization of the siderophore receptor FhuA, integral outer membrane protein from *Escherichia coli* K-12. *Protein Sci.* **7:** 1636–1638.

Ferguson, A.D., Hofmann, E., Coulton, J.W., Diederichs, K., and Welte, W. 1998b. Siderophore-mediated iron transport: Crystal structure of FhuA with bound lipopolysaccharide. *Science* **282:** 2215–2220.

Ferguson, A.D., Chakraborty, R., Smith, B.S., Esser, L., van der Helm, D., and Deisenhofer, J. 2002. Structural basis of gating by the outer membrane transporter FecA. *Science* **295:** 1715–1719.

Hantke, K. 1981. Regulation of ferric iron transport in *Escherichia coli* K12: Isolation of a constitutive mutant. *Mol. Gen. Genet.* **182:** 288–292.

Howard, S.P., Herrmann, C., Stratilo, C.W., and Braun, V. 2001. In vivo synthesis of the periplasmic domain of TonB inhibits transport through the FecA and FhuA iron siderophore transporters of *Escherichia coli*. *J. Bacteriol.* **183:** 5885–5895.

Khursigara, C.M., De Crescenzo, G., Pawelek, P.D., and Coulton, J.W. 2004. Enhanced binding of TonB to a ligand-loaded outer membrane receptor: Role of the oligomeric state of TonB in formation of a functional FhuA-TonB complex. *J. Biol. Chem.* **279:** 7405–7412.

Khursigara, C.M., De Crescenzo, G., Pawelek, P.D., and Coulton, J.W. 2005. Kinetic analyses reveal multiple steps in forming TonB–FhuA complexes from *Escherichia coli*. *Biochemistry* **44:** 3441–3453.

Killmann, H., Benz, R., and Braun, V. 1993. Conversion of the FhuA transport protein into a diffusion channel through the outer membrane of *Escherichia coli*. *EMBO J.* **12:** 3007–3016.

Killmann, H., Videnov, G., Jung, G., Schwarz, H., and Braun, V. 1995. Identification of receptor binding sites by competitive peptide mapping: Phages T1, T5, and ϕ 80 and colicin M bind to the gating loop of FhuA. *J. Bacteriol.* **177:** 694–698.

Killmann, H., Herrmann, C., Torun, A., Jung, G., and Braun, V. 2002. TonB of *Escherichia coli* activates FhuA through interaction with the β-barrel. *Microbiol.* **148:** 3497–3509.

Kim, M., Fanucci, G.E., and Cafiso, D.S. 2007. Substrate-dependent transmembrane signaling in TonB-dependent transporters is not conserved. *Proc. Natl. Acad. Sci.* **104:** 11975–11980.

Locher, K.P., Rees, B., Koebnik, R., Mitschler, A., Moulinier, L., Rosenbusch, J.P., and Moras, D. 1998. Transmembrane signaling across the ligand-gated FhuA receptor: Crystal structures of free and ferrichrome-bound states reveal allosteric changes. *Cell* **95:** 771–778.

Mandava, S., Makowski, L., Devarapalli, S., Uzubell, J., and Rodi, D.J. 2004. RELIC—a bioinformatics server for combinatorial peptide analysis and identification of protein-ligand interaction sites. *Proteomics* **4:** 1439–1460.

Moeck, G.S. and Letellier, L. 2001. Characterization of in vitro interactions between a truncated TonB protein from *Escherichia coli* and the outer membrane receptors FhuA and FepA. *J. Bacteriol.* **183:** 2755–2764.

Moeck, G.S., Ratcliffe, M.J., and Coulton, J.W. 1995. Topological analysis of the *Escherichia coli* ferrichrome-iron receptor by using monoclonal antibodies. *J. Bacteriol.* **177:** 6118–6125.

Moeck, G.S., Tawa, P., Xiang, H., Ismail, A.A., Turnbull, J.L., and Coulton, J.W. 1996. Ligand-induced conformational change in the ferrichrome-iron receptor of *Escherichia coli* K-12. *Mol. Microbiol.* **22:** 459–471.

Moeck, G.S., Coulton, J.W., and Postle, K. 1997. Cell envelope signaling in *Escherichia coli*. Ligand binding to the ferrichrome-iron receptor FhuA promotes interaction with the energy-transducing protein TonB. *J. Biol. Chem.* **272:** 28391–28397.

Moreau, V., Granier, C., Villard, S., Laune, D., and Molina, F. 2006. Discontinuous epitope prediction based on mimotope analysis. *Bioinformatics* **22:** 1088–1095.

Myszka, D.G. 1999. Improving biosensor analysis. *J. Mol. Recognit.* **12:** 279–284.

Pawelek, P.D., Croteau, N., Ng-Thow-Hing, C., Khursigara, C.M., Moiseeva, N., Allaire, M., and Coulton, J.W. 2006. Structure of TonB in complex with FhuA, *E. coli* outer membrane receptor. *Science* **312:** 1399–1402.

Quinn, J.G. and O'Kennedy, R. 2001. Biosensor-based estimation of kinetic and equilibrium constants. *Anal. Biochem.* **290:** 36–46.

Scott, D.C., Newton, S.M., and Klebba, P.E. 2002. Surface loop motion in FepA. *J. Bacteriol.* **184:** 4906–4911.

Shultis, D.D., Purdy, M.D., Banchs, C.N., and Weiner, M.C. 2006. Outer membrane active transport: Structure of the BtuB:TonB complex. *Science* **312:** 1396–1399.

Stoye, J., Moulton, V., and Dress, A.W. 1997. DCA: An efficient implementation of the divide-and-conquer approach to simultaneous multiple sequence alignment. *Comput. Appl. Biosci.* **13:** 625–626.

Yelton, D.E., Desaymard, C., and Scharff, M.D. 1981. Use of monoclonal anti-mouse immunoglobulin to detect mouse antibodies. *Hybridoma* **1:** 5–11.

Yue, W.W., Grizot, S., and Buchanan, S.K. 2003. Structural evidence for iron-free citrate and ferric citrate binding to the TonB-dependent outer membrane transporter FecA. *J. Mol. Biol.* **332:** 353–368.

Zhang, C.W., Chishti, Y., Hussey, R.E., and Reinherz, E.L. 2001. Expression, purification, and characterization of recombinant HIV gp140. The gp41 ectodomain of HIV or simian immunodeficiency virus is sufficient to maintain the retroviral envelope glycoprotein as a trimer. *J. Biol. Chem.* **276:** 39577–39585.